LAVA FLOODING OF ANCIENT PLANETARY CRUSTS: GEOMETRY, THICKNESS, AND VOLUMES OF FLOODED LUNAR IMPACT BASINS

JAMES W. HEAD

Department of Geological Sciences, Brown University, Providence, Rhode Island, U.S.A.

(Received August 12, 1981)

Abstract. Estimates of lava volumes on planetary surfaces provide important data on the lava flooding history and thermal evolution of a planet. Lack of information concerning the configuration of the topography prior to volcanic flooding requires the use of a variety of techniques to estimate lava thicknesses and volumes. A technique is described and developed which provides volume estimates by artificially flooding unflooded lunar topography characteristic of certain geological environments, and tracking the area covered, lava thicknesses, and lava volumes. Comparisons of map patterns of incompletely buried topography in these artificially flooded areas are then made to lava-flooded topography on the Moon in order to estimate the actual lava volumes.

This technique is applied to two areas related to lunar impact basins; the relatively unflooded Orientale basin, and the Archimedes–Apennine Bench region of the Imbrium basin. Artificially flooding the Orientale basin to the Cordillera Mountains (outer basin ring) produces a lava fill geometry with two components; (a) the *basin interior* (within the inner Rook ring) where the area covered is small but lava thicknesses are large (6–8 km), and (b) the *basin edges* where larger areas are covered but thicknesses are less, averaging about 2 km. Detailed examination of the Archimedes–Apennine Bench area (Imbrium basin edge) also shows average thicknesses in this region of basins of approximately 2 km.

On the basis of these analyses it is concluded that early flooding of the basin interior places a major load on the lithosphere in the same geographic region where mascon gravity anomalies are concentrated. Mare ridges and arches are concentrated at the outer edge of the region of thickset fill and appear to be related to tectonic activity accompanying basin loading and downwarping. Lava thicknesses in most areas of flooded impact basins (> 2 km) exceed the thickness of lava where vertical mixing of underlying non-mare material is possible. Thus, vertical mixing is not likely to have been an important process in mare deposits within flooded impact basins. Thickness estimates derived from this technique exceed those derived from the morphometry of buried or partially buried craters by at least a factor of two. Examination of the assumptions employed in the latter technique show several sources of variability (e.g., initial rim height variability in a fresh crater) which may result in significant underestimation of lava thicknesses.

1. Introduction

Recognition of the volcanic origin of surface deposits on ancient cratered planetary surfaces provides important information on the presence and significance of melting in the interior. Establishment of the composition, age, and volume of such deposits provides additional clues concerning the characteristics of the thermal history of the planet. In addition, the thickness, geometry, and volumes of volcanic deposits provide important data for understanding sources and styles of volcanism and relationship between tectonics and lithospheric deformation (Solomon and Head, 1979, 1980). Only a portion of the magma generated at depth, however, is extruded out to the surface. Some may remain

The Moon and the Planets **26** (1982) 61–88. 0165–0807/82/0261–0061$04.20.

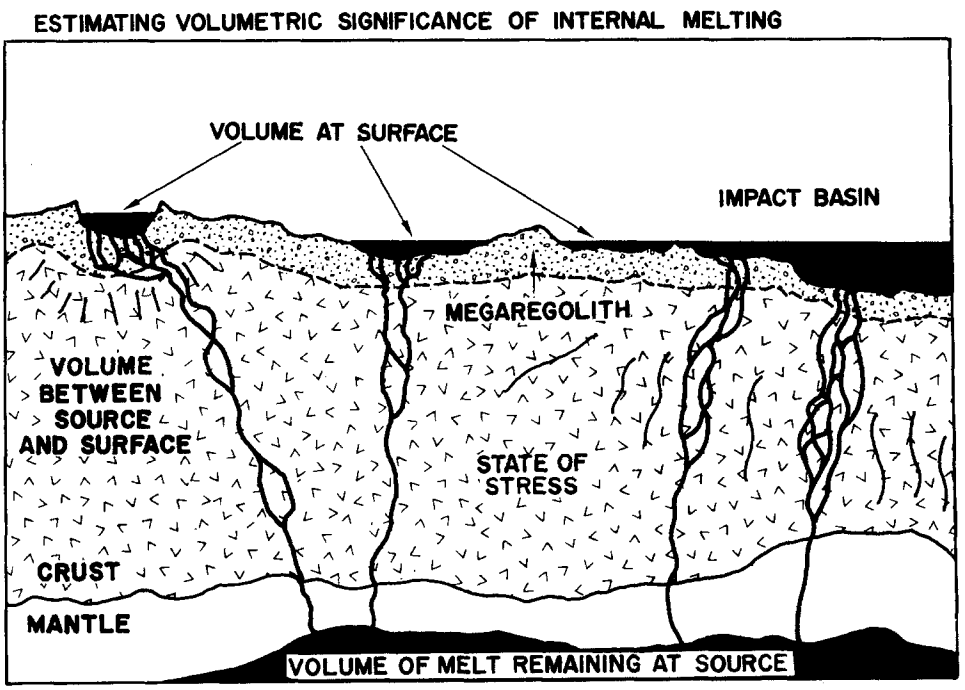

Fig. 1. Estimates of the volumetric significance of internal melting. Only a portion of the magma generated at depth reaches the surface. Some portion remains at the source and a quantity is intruded between the source and surface. The state of stress in the crust or lithosphere is a factor in determining volcanic style.

at the source and some quantity is intruded between the source and surface (Figure 1). Documentation of the quantities reaching the surface is an important first step in reaching the objectives outlined above. This study concentrates on determining the geometry, thickness, volumes, and style of emplacement of lavas extruded onto an ancient planetary crust (Head, 1979a, b), with particular emphasis on crustal regions characterized by the topography of impact basins.

Once deposits have been recognized as of volcanic origin, it has often been difficult to establish thicknesses and volumes because in the processes of emplacement, lavas cover the initial crustal surface, obscuring the geometry of the pre-volcanic terrain. Attempts to establish thicknesses and volumes have concentrated on four basic approaches (Figure 2):

1.1. CRATER MORPHOMETRY

Measuring diameters and exposed rim heights of impact craters protruding through the deposits (Marshall, 1961; Baldwin, 1970; DeHon, 1974, 1975, 1977, 1979a, b, c; DeHon and Waskom, 1976, Hörz, 1978). The basic principle is that a fresh impact crater represents a landform displaying characteristic size relationships between various morphologic features such as crater interior, rim, and floor (Pike, 1977, 1978). Thus a measurement of

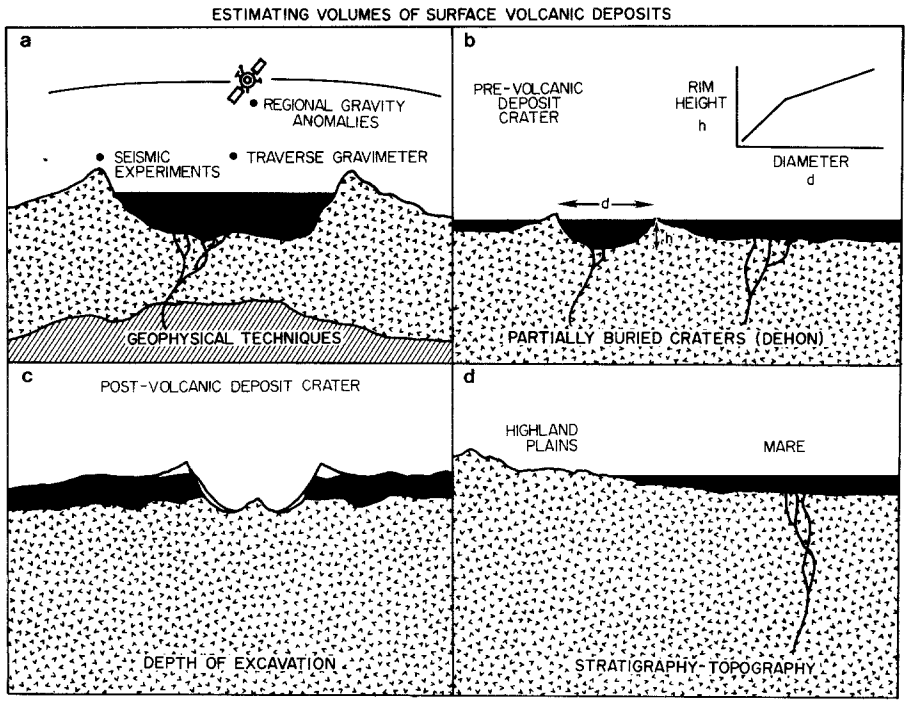

Fig. 2. Four basic approaches for determining lava thicknesses and volumes. (a) Geophysical techniques. (b) Crater morphometry. (c) Crater penetration. (d) Stratigraphic and topographic relationships.

the diameter of a crater rim crest just protruding through the lava deposits can be related to the crater depth or to the height of the rim crest above surrounding terrain before flooding (Figure 2b). Caution must be exercised in applying this technique for two reasons: (a) the measured crater may not be fresh. If the crater is degraded, the rim height (and lava thickness) will be overestimated (Hörz, 1978). This effect may tend to be offset by the fact that much lava flooding on the Moon occurs in relatively young impact basins (Imbrium, Crisium, Serenitatis). Since the formation of these basins destroys preexisting craters within the basin interior, the craters forming after basin formation and before lava flooding should be relatively fresh, and rim degradation minimized; (b) the measured crater may have formed *during* the lava emplacement, resulting in an underestimate of total lava thickness. Use of numerous data points will tend to minimize these effects and show regional thickness relationships (DeHon, 1974).

1.2. Crater Penetration

Locating craters in volcanic deposits that post-date the lavas, and penetrate through them, and using the crater depth as a measure of lava thickness (Figure 2c). Remote sensing data can be used to determine that the crater interior or ejecta deposit is derived from underlying terrain, producing a maximum thickness estimate (Andre *et al.*, 1979; Head *et al.*,

1978). Similarly, if the ejecta is of mare composition only, then the crater depth may give a minimum estimate of lava thickness. Uncertainty about the processes involved in crater cavity formation and modification (Settle and Head, 1979) make exact thickness estimates difficult. For example, extensive central uplift (Grieve *et al.*, 1977; Grieve, 1980) in craters not actually penetrating through the maria can expose material in the central peaks that originally lay well below the maximum depth of excavation. The assumption that the crater had actually penetrated through the lava deposit would lead to an underestimate of lava thickness.

1.3. STRATIGRAPHY

(Figure 2d). Stratigraphic techniques and regional topography can be used to estimate lava thicknesses, particularly at the edge of lava deposits, where topography and onlap relationships are clear (Head, 1974a).

1.4. GEOPHYSICAL TECHNIQUES

(Figure 2a). Surface geophysical techniques include the traverse gravimeter, which estimated a lava thickness of 1 km at the Apollo 17 site (Talwani *et al.*, 1973), and active seismic experiments, which estimated a thickness of ~ 1.4 km at the Apollo 17 site (Cooper *et al.*, 1974). Gravity anomalies in mascon basins can be converted to lava volumes and thicknesses (Solomon and Head, 1979, 1980). Similar techniques can be applied to the irregular maria (Thurber and Solomon, 1978). These latter techniques provide lower bounds for the thickness of lunar mare basalt fill of 3 km in mascon maria and 0.5–1.5 in irregular maria (Thurber and Solomon, 1978).

Although these approaches have provided significant advances in the understanding of the emplacement of the lunar maria (DeHon and Waskom, 1976), there are still basic uncertainties concerning thicknesses and volumes in many areas. The major difficulty in establishing thicknesses and volumes in flooded areas is reconstructing the sub-volcanic topography. Greeley and Womer (1980) and Womer and Greeley (1981) have simulated lava flooding of a basin using scale models in the laboratory. The approach taken here, however, is to start with *known* topography characteristic of early planetary crusts, and to artificially flood it with lava, keeping track of the evolving thickness, volume, surface area covered, and map pattern. Upon completion of flooding (no sub-volcanic topography exposed), data are available on maximum and average lava thicknesses, total volume, and the relationship of area covered (or exposed) to lava thickness and volume. In addition, a series of maps is available to show patterns of exposed sub-volcanic topography at various stages of filling. Since the volume and thickness of lavas associated with each map pattern is known, these maps can be used to estimate the same parameters for flooded planetary areas that show comparable map patterns. A range of unflooded terrain typical of early planetary crusts is being investigated (highland cratered terrain; basin interiors; basin margins; large craters; upland plains). This paper reports on the results of experiments in several areas of lunar basin interiors and margins.

The procedure is as follows: Lunar Topographic Orthophotomaps (1:250 000), Lunar

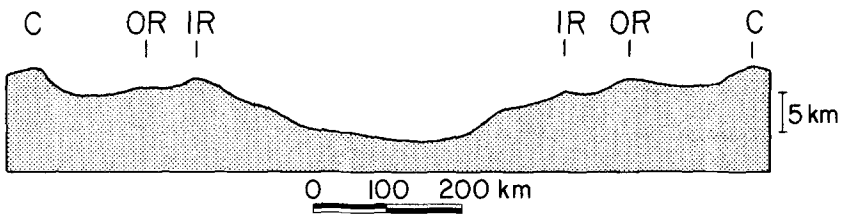

Fig. 3. Topographic profile of unflooded Orientale basin. Profile extends from south (left) to north (right). Vertical exaggeration X 10. Derived from Watts limb measurements compiled in Head *et al.* (1981). C = Cordillera, OR = Outer Rook, and IR = Inner Rook Mountains.

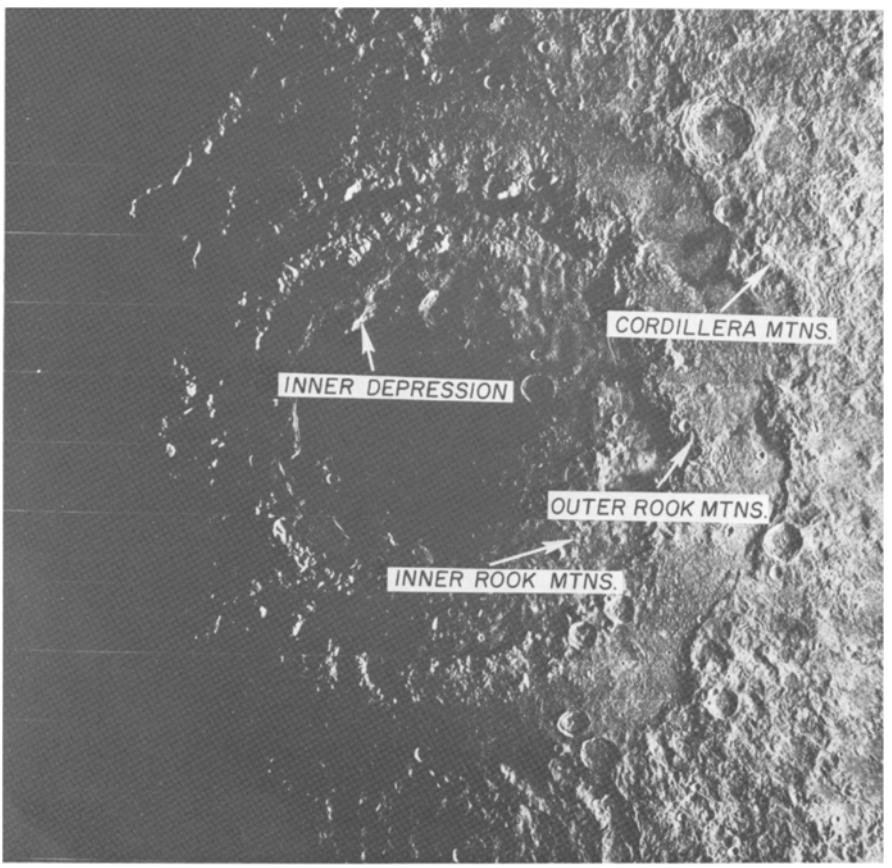

Fig. 4(a)

Maps (1:1 000 000) and other contour maps are used as base maps. The contours of each map chosen are digitized at designated intervals. For this study the assumption is made that lava sources are ubiquitous; thus flooding begins at the lowest point on the map, flooding evenly to each new contour level, and begins in separate isolated depressions as the rising lava first encounters the appropriate contour within the depression. Flooding continues until all topography disappears. Lava thickness as a function of area and volume are plotted, and maps of any stage of flooding can be produced by Calcomp plots of the digitized topographic data. Data reduction techniques are described in Appendix A.

One of the major difficulties in determining volcanic deposit thicknesses in many lunar maria is the fact that the deposits occupy relatively young lunar basins. The relative youth of the basins means (1) that there are fewer post-basin craters that can be used to determine basalt thickness by conventional methods, and (2) that the geometry of the young basins is sufficiently deep so that many craters are completely covered. The purpose of this paper is to report on the artificial flooding of two basin-related areas in order to obtain thickness and volume estimates for multi-ringed basins flooded by mare deposits.

The major topography of young multi-ringed basins, as revealed by the relatively unflooded Orientale basin (Moore *et al.*, 1974; Head, 1974b; Head *et al.*, 1975; Howard *et al.*, 1974; Head *et al.*, 1981) consists of an inner depression and rough topography comprised of basin rings and associated facies within the major scarp defining the basin (the Cordillera Mountains for Orientale) (Figures 3, 4a). Some basins are flooded out to the outer scarp (Imbrium, in many places, for example; Wilhelms and McCauley, 1971), others are flooded only to the major second ring (Serenitatis [Head, 1978]), while others are flooded primarily in the inner depression (Orientale [Greeley, 1976] and Nectaris). Two separate areas are treated here: the *Orientale basin*, and the *Archimedes–Apennine Bench region* which represents the region between the second and third basin rings in Imbrium.

2. The Orientale Basin Example

Topography for the Orientale basin was derived from a series of limb profiles (Watts, 1963) and is consistent with topography determined from other sources (Head, 1974b; Howard *et al.*, 1974; Brown *et al.*, 1974; Kaula *et al.*, 1974). A topographic map of Orientale was produced using the Watts limb measurements and contouring the data points for elevations (Head *et al.*, 1981). Data exist for only slightly over half the basin; this topography was assumed to be characteristic of the rest of the basin and the values in Figures 4e, f reflect flooding of the whole basin. Since the basin interior is known to vary in morphology from east to west (Moore *et al.*, 1974), actual topographic data from the west would undoubtedly modify details of the curves, but the general shapes would very likely remain the same. The interior of Orientale (Figure 4a) contains maria perhaps up to one km thick (Head, 1974a; Greeley, 1976; Scott *et al.*, 1977) and several thinner patches of maria at the base of the second and third rings (Greeley, 1976; Gaddis and Head, 1981).

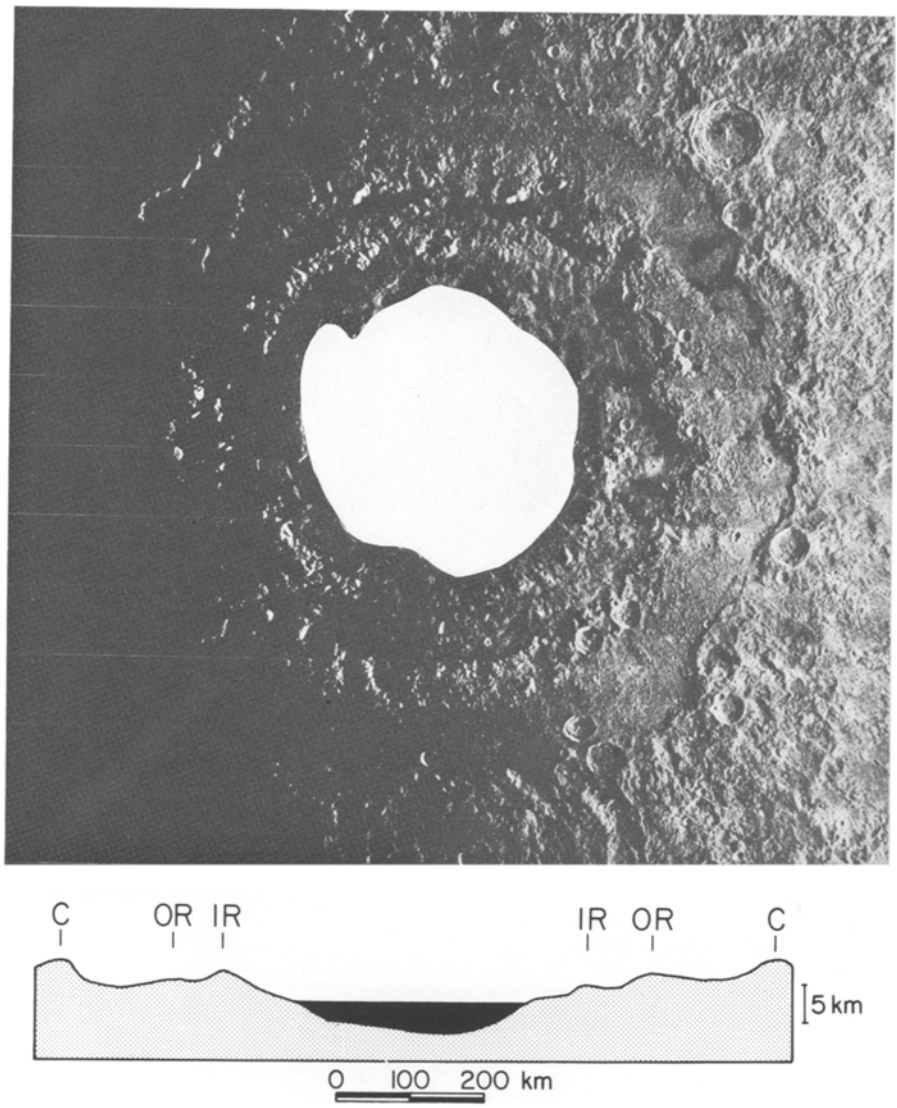

Fig. 4(b)

Using the computer-generated topographic map derived from the limb data (Head *et al.*, 1981), the present topography was flooded and the volumes and area covered were tracked at one kilometer intervals. The area covered as a function of each additional km is shown in Figure 4e. The flooding takes place in two major stages. When the inner depression of Orientale (about 80×10^3 km^2) is flooded the deposits are characterized by a maximum lava thickness of between 3 and 4 km (Figures 4b, 4e) and a lava volume of $100–200 \times 10^3$ km^3 (Figure 4f). When the flooding reaches the inner Rook Mountain

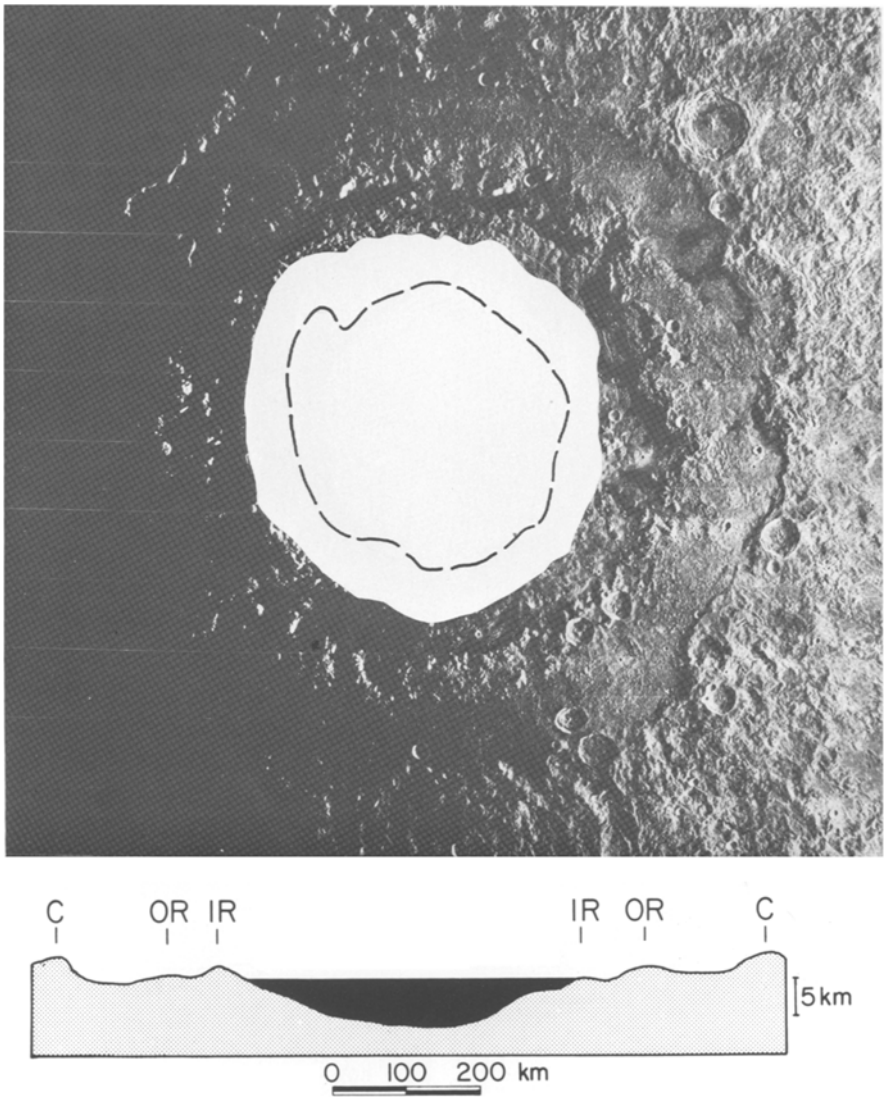

Fig. 4(c)

ring (peak ring) an area of about 180×10^3 km^2 is covered and an additional 2 km of lava added (Figures 4c, e). In this first stage of flooding the emphasis is on filling of the pronounced inner topographic depression: three-fourths of the total thickness is added during this stage (about 6 km) (Figure 4e); however, less than one-third of the total area and less than one-half the total volume are added (Figure 4f). The second stage of basin fill emphasizes the flooding of the region between the inner Rook Mountains and the basin-defining scarp (Cordillera Mountains) (Figure 4d). An additional two kilometers is

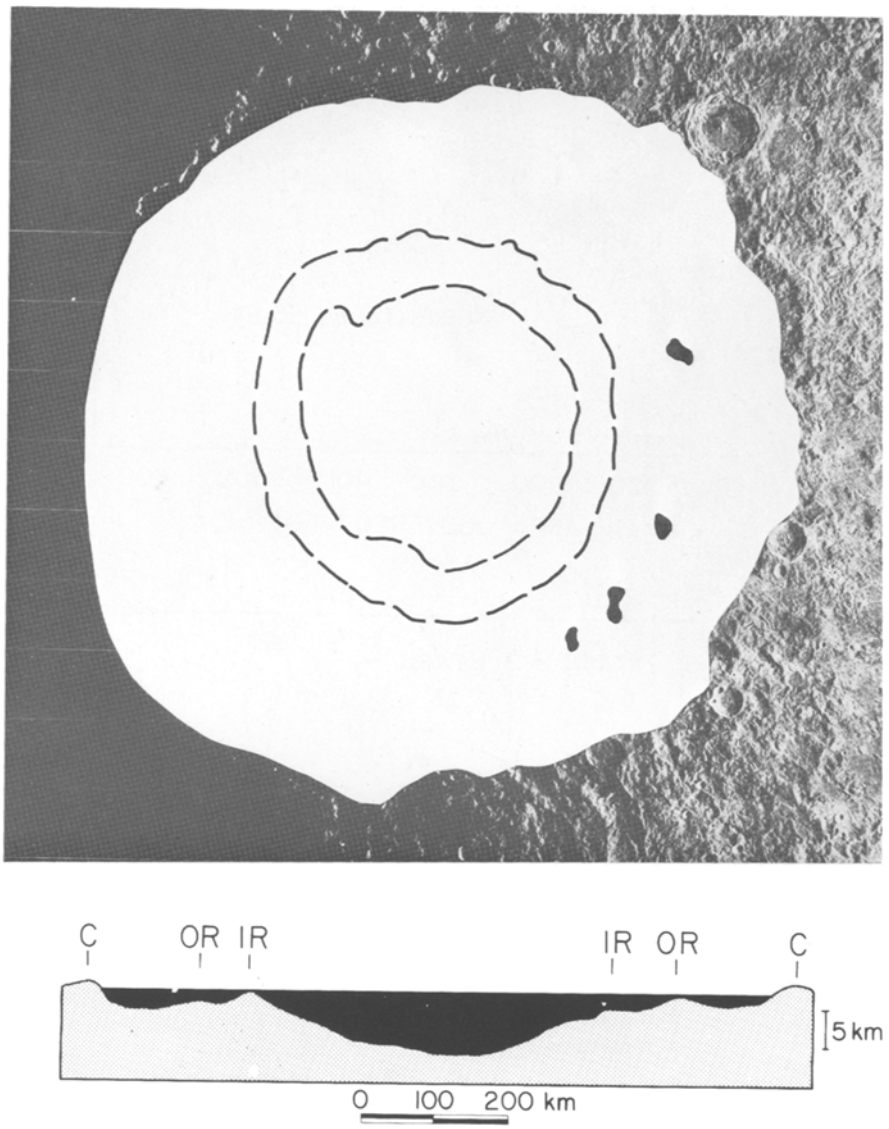

Fig. 4(d)

required to flood the basin to the Cordillera ring (Figure 4d). At this point only a few peaks are present in the basin interior and parts of the Cordillera ring are flooded (the map pattern is similar to that seen in southern Mare Imbrium in the Carpathian Mt.–Copernicus region). The addition of these two kilometers triples the area covered by lava, and doubles the volume of lava in the basin (Figures 4e, f). An isopach map of the flooded Orientale basin is shown in Figure 5.

Analysis of the flooding history of Orientale outlined above indicates the following:

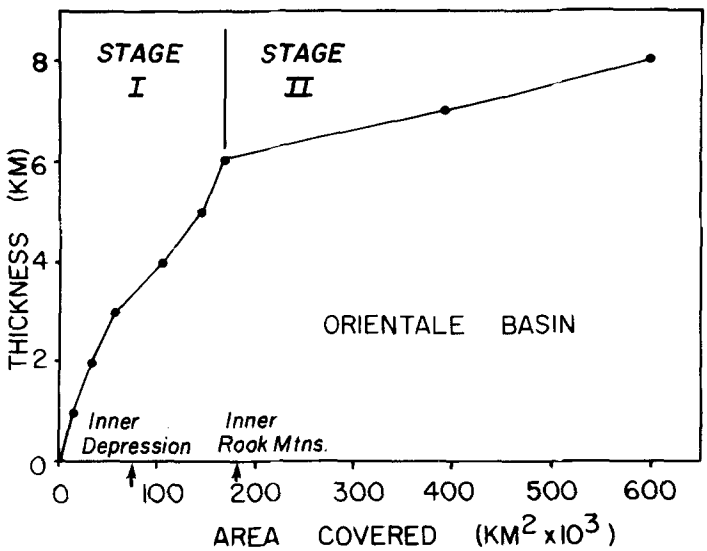

Fig. 4(e)

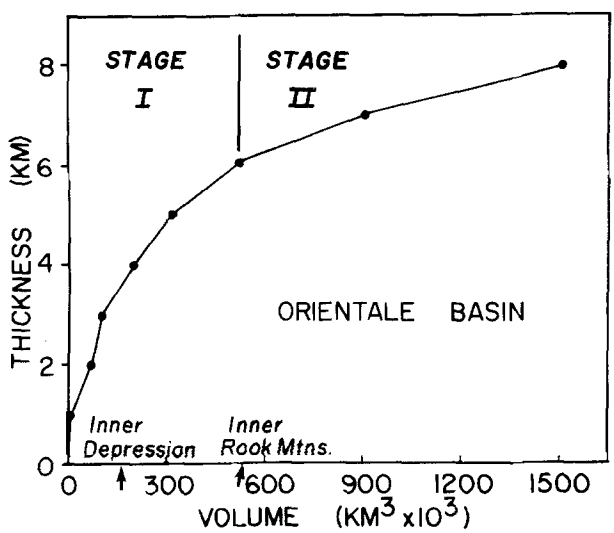

Fig. 4(a–f). Flooding of Orientale basin. Photographs and topographic profiles illustrate lava thickness and area covered at various stages of flooding. (a) Orientale basin with interior features labelled. (b) Early Stage I flooding of the inner depression. (c) Basin at completion of Stage I flooding. Lava reaches the base of the Inner Rook Mountains (peak ring). Dashed lines mark the extent of earlier Stage I flooding. (d) Basin at completion of Stage II flooding. Lava reaches the Cordillera Mountains (outer ring). Dashed lines mark extent of Stage I flooding. Black spots represent peaks of the Outer Rook Mountains protruding through the lava fill. (e) Area covered as a function of thickness. Early flooding is characterized by large lava thicknesses and small area covered whereas later flooding is characterized by smaller lava thicknesses and a much greater area covered. (f) Volume of lava accumulated as a function of thickness. Large lava thicknesses and small to intermediate volumes are characteristic of early flooding whereas small lava thicknesses and intermediate to large volumes are characteristic of later flooding.

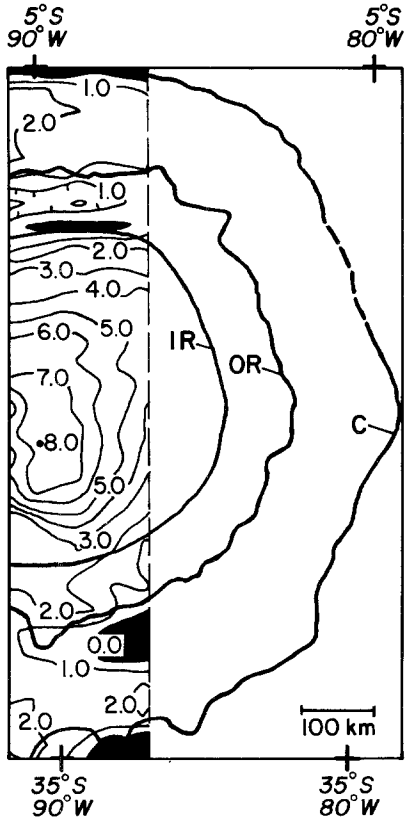

Fig. 5. Isopach map of the flooded Orientale basin. Stage I and Stage II flooding episodes result in total lava thicknesses of up to 8 km (in addition to the 1 km of lava present prior to flooding [Head, 1974a; Greeley, 1976]). Lava thickness contour interval is 1.0 km. Isopach map covers the portion of Orientale basin where topography is most reliable. Traces of basin rings are indicated by heavy black lines. Solid black areas are regions above the surface flooded to 8 km thickness.

2.1. STYLE OF FLOODING

Early flooding of the basin interior (Stage I) is characterized by large lava thickness, small area covered, and small to intermediate volumes (less than one-half of the total fill volume). Later flooding (Stage II) is characterized by small lava thickness, large area covered, and intermediate to large volumes (over one-half the total fill volume). As shown by the actual mare deposits in Orientale (Figure 4a) (Greeley, 1976; Gaddis and Head, 1981), lavas may be initially emplaced along the margins of the basin as well as in the interior. However, the geometry of the basin is such that initial large volumes of lava will be concentrated in the basin interior even if their sources lie along the edges of the outer basin scarps. For a given eruption volume, early deposits are likely to be thicker and concentrated in a smaller area, while later deposits will tend to be thinner and more widespread.

2.2. GEOMETRY OF DEPOSITS AND IMPLICATIONS FOR LOADING OF THE LITHOSPHERE

The resulting Stage I deposit has the approximate geometry of an inverted truncated cone with a basal radius to height ratio of about 40:1. The resulting Stage II deposit has the approximate geometry of a thin disc with a radius to height ratio of about 225:1. Detailed studies of basin mare stratigraphy (Howard *et al.*, 1974; Sharpton and Head, 1981a) show that the actual emplacement history of mare basalts is not exactly comparable to the simplified stages and geometry indicated above because of variable source locations and the subsidence of the basin in response to early lava loads (Solomon and Head, 1979, 1980). However, the emplacement history and geometry is known sufficiently to make the following observations:

(a) the early load will tend to be concentrated in the basin interior, the region where the observed mascon masses appear concentrated (Phillips *et al.*, 1972);

(b) since the lithosphere is thickening with time, it will respond most readily to loads applied early. Thus, downwarping of the basin should be accelerated and concentrated in the basin interior during early stages of fill;

(c) concentric mare arches and ridges are often developed within filled mare basins and their location approximates the position of the basin peak ring. The location of these ridges may be related to differential vertical movement at the edge of the Stage I load (see also DeHon and Waskom, 1976). An additional possible explanation is that the flooded peak ring acts as a stress concentrator related to local or regional stresses. Evidence for differential vertical movement is seen in the Crisium basin where a subsurface stratigraphic discontinuity exists in this part of the basin (Head *et al.*, 1978; Peeples *et al.*, 1978; Maxwell and Phillips, 1978). A similar situation is seen in Mare Serenitatis where mare arches occur over the peak ring (Head, 1978; Sharpton and Head, 1981a, b).

(d) If fresh basins begin with a morphology and morphometry similar to Orientale (Figure 4a), the presence of peak ring remnants may be a measure of downwarping. For relatively fresh but flooded basins, the presence of portions of the peak ring (Figures 4a, d) implies that downwarping of the basin due to the load is not sufficient to cover them during Stage II flooding. In degraded basins, however, the peak rings may be heavily subdued at the time of lava flooding.

2.3. LAVA THICKNESS AND VERTICAL MIXING

The maximum thickness of lava in the artifically flooded Orientale basin at the end of Stage II is 8 km. This is a minimum estimate since about one km of lava presently exists in the basin and downwarping due to loading during filling was not taken into account. The percentage of the basin covered by different lava thicknesses is shown in Figure 4e. An important question related to the presence of non-mare components in soils collected at Apollo mare sites is whether or not these non-mare materials might be derived from *vertical* mixing of sub-mare materials by impact processes. Hörz (1978) indicates that thicknesses greater than one km would preclude significant vertical mixing by impact processes. One hundred percent of the basin within the inner Rook Mountains exceeds this depth, and about one-half of the rest of the basin fill is thicker than one km. Vertical

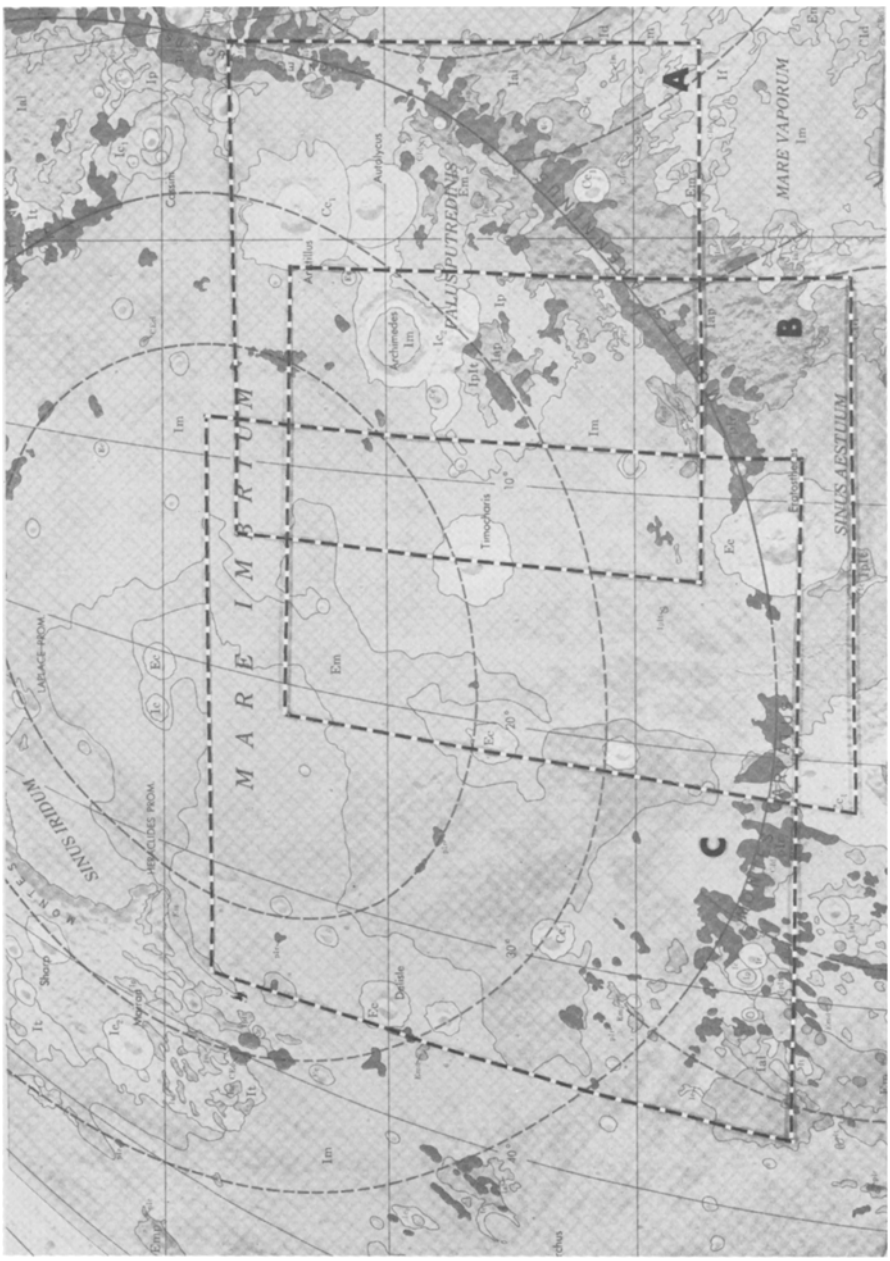
MARE IMBRIUM
PALUS PUTREDINIS
MARE VAPORUM
SINUS AESTUM
SINUS IRIDUM
A
B
C
Archimedes
Aristillus
Autolycus
Timocharis
Eratosthenes
Delisle
Sharp
Newton
LAPLACE-PROM
HERCULES PROM

Fig. 6 (a)

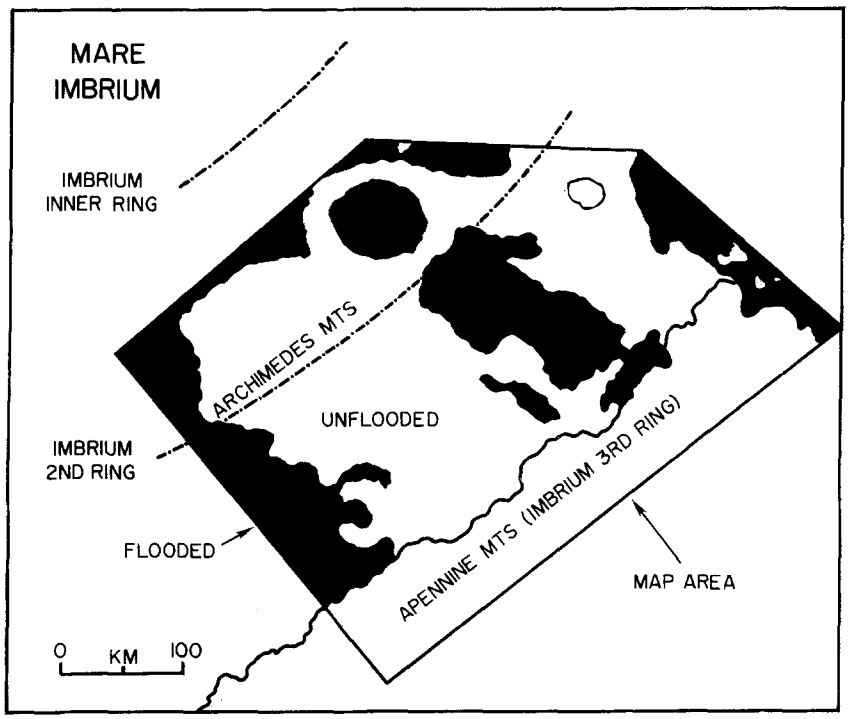

Fig. 6(a–b). Mare Imbrium. (a) Location of areas shown in Figures 6(b) and 10. (b) Archimedes–Apennine Bench region (area A of Figure 6(a) showing locations of Imbrium basin rings and area presently covered by maria. Region designated as map area is region of artificial flooding.

mixing could only have been significant in the earliest stages of fill in Stage II. The inner depression probably filled to one km depth relatively rapidly, although the flux was higher at the time. Detailed consideration of the possibility of vertical mixing in regions covered during Stage II is presented in the next section.

3. The Archimedes–Apennine Bench Example

A further assessment of the second stage of fresh basin flooding can be obtained by analysis of the *Archimedes–Apennine Bench region*. This is a relatively unflooded region of the Imbrium basin lying between the second ring and the outer (third) Apennine Mountain ring (Figures 6a, b). Some mare deposits exist in the area and the region may have been the site of post-Imbrium, pre-mare volcanism (Hawke and Head, 1978; Spudis, 1978); thus, estimates for lava filling are probably conservative. A region centered on Palus Putredinis (NASA Map LM41, MONTES APENNINUS, 1:1M Scale) was artificially flooded at 300 m intervals using procedures described for Orientale and in Appendix A. The area covered and volume accumulated as a function of thickness are plotted in Figures 7a, b.

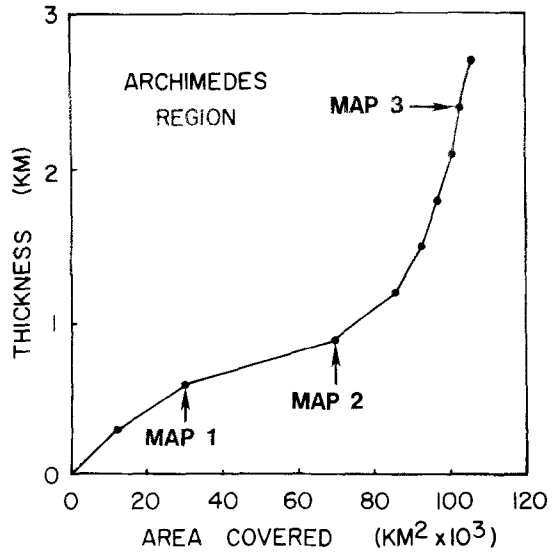

Fig. 7(a)

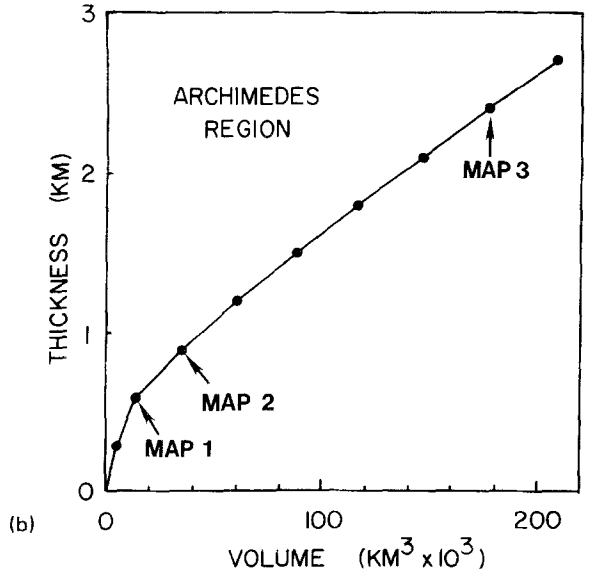

Fig. 7(a–b). Thickness, area, and volume relationships for the artificially flooded Archimedes–Apennine Bench region. Map number designations correspond to maps shown in Figure 8. (a) Area covered as a function of lava thickness. (b) Volume accumulated as a function of lava thickness.

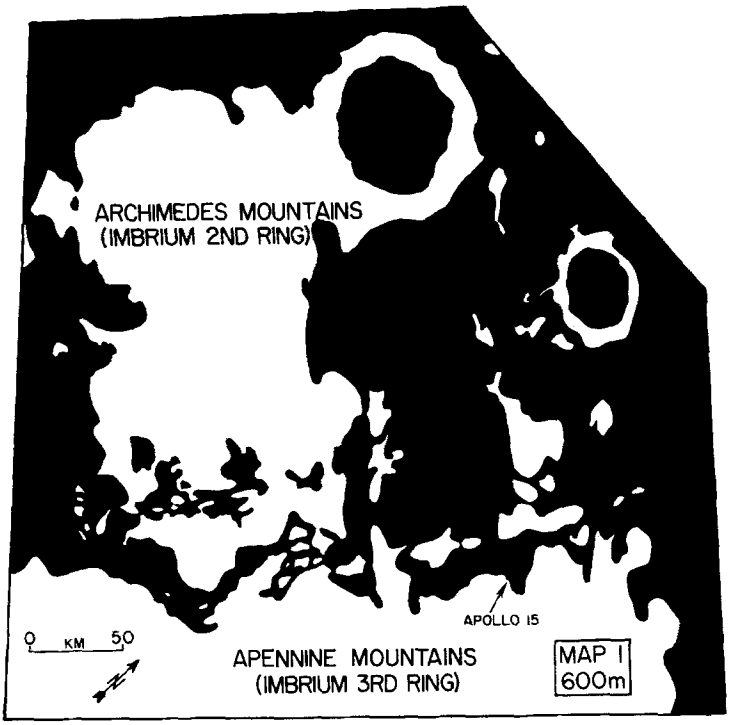

Fig. 8(a)

The addition of 600 m of lava (Map 1, Figure 8a) changes the map pattern by adding lava along the base of the Apennine Mountain front and the area east of Archimedes. A very small volume increase covers over 25% of the unflooded area (Figure 7a, b). The average lava thickness of the newly flooded area is 485 m. An additional 300 m of lava (Map 2; Figure 8b) continues the flooding trend shown in Map 1; that is, a small additional volume increase (~ 10% of total volume), covers an additional 35% of the area. The craters Archimedes and Autolycus are isolated so that only their rim crests are exposed. The major topography between the second and third ring is being covered, particularly toward the base of the Apennines. The average thickness at this point is slightly over 500 m.

Considerable additional thickness is required to cover the mountain peaks associated with the second ring (Archimedes Mts.). These are equivalent to the outer Rook Mountain in the Orientale basin (Figures 4a, 5). Map 3 (Figure 8c) illustrates the pattern after 2400 m of lava have been added (Figures 7a, b). Although only the tip of the Archimedes Mountains remains exposed, an additional 700 m would be required to cover them completely. The *average* thickness is 1.74 km. On the basis of the flooding history, an isopach map of the region was prepared (Figure 9). At the termination of flooding, several small areas of Montes Archimedes (standing 200–400 m above the surrounding plain) and the vast majority of the Apennine Mountains remain unflooded. Total thickness to flood to

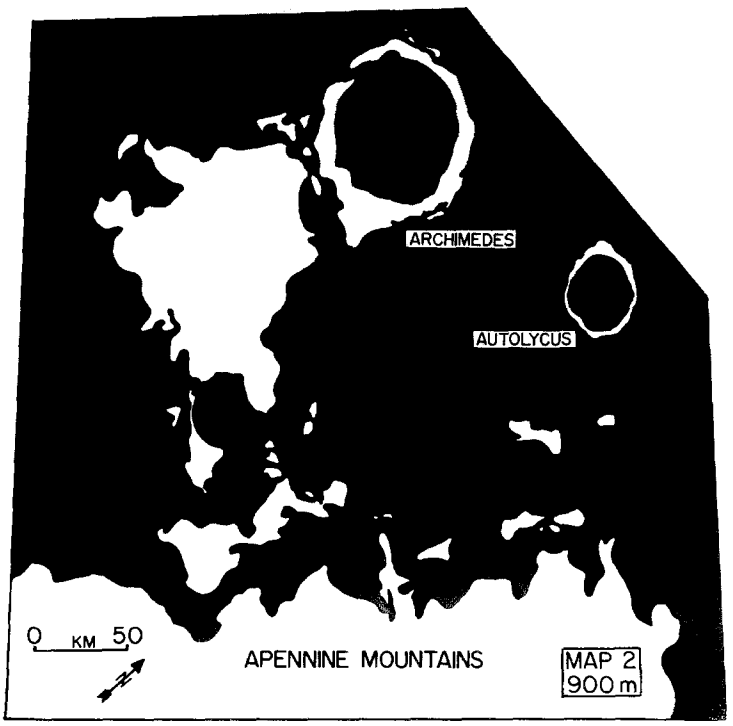

Fig. 8(b)

this level is 2.7 km. Average thickness of lava (total volume/total area) is 1.99 km. An additional 3 km of lava would be required to cover the Apennine Mountains.

What areas in Mare Imbrium are comparable to the artificially flooded region? Figure 6a shows the location of two regions in south central and southwestern Mare Imbrium which appear comparable to the Apennine test area flooded to the level of Map 3 (Figure 8c). In the region between Archimedes and Copernicus, no portion of the second ring is exposed (Figure 10a) and the extension of the Apennine ring (Montes Carpatus) appears morphologically similar to the deeply incised Apennines of Map 3 (Figure 8c). To the west (Area C, Figure 10b) some subjacent topography is exposed southwest of Euler.

DeHon (1979a) has published an isopach map for the Imbrium region (Figure 11) prepared on the basis of the morphometry of buried craters. The diameter of flooded (ghost) or partially flooded (protruding rim) craters is measured; the average exterior rim height of fresh craters is known from the work of Pike (1977; 1978). If the crater is buried, the rim height provides a minimum thickness value; if the rim protrudes, the present rim elevation is subtracted from the average value for a fresh crater of the same diameter, yielding a thickness value. The data points are then contoured to produce the isopach map. DeHon's map of Imbrium (Figure 11) shows thicknesses in the southern Imbrium region which are less than the values proposed in this paper by a factor of two or three. What are the potential causes of discrepancies between these two techniques?

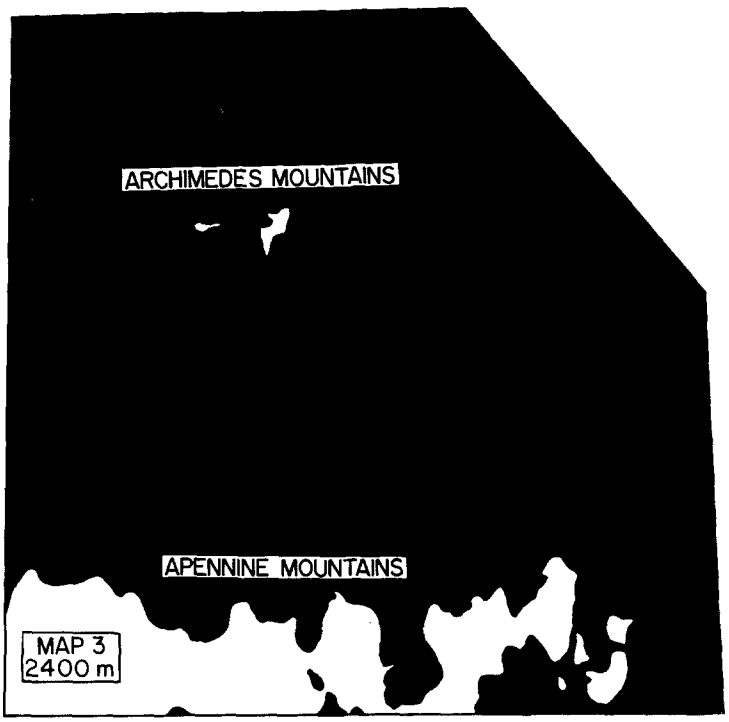

Fig. 8(a–c). Maps of the Archimedes–Apennine Bench region illustrating flooding patterns for various lava thickness intervals. (a) 600 m; (b) 900 m; (c) 2400 m.

3.1. NUMBER OF DATA POINTS

As DeHon (1979a, c) points out, the number of data points within young circular basins is small because of the reduced flux characteristic of post-basin times and the thicker basalts found in basin interiors. For the southern Imbrium region, DeHon's isopach map is based on seven data points (Table I; Figure 11). The Archimedes–Apennine Bench example outlines above however provides lava thickness estimates for the whole sample region.

3.2. RIM HEIGHTS OF FRESH LUNAR CRATERS

Hörz (1978) has pointed out that crater rim crests can undergo rapid degradation without significant change in crater diameter. He further points out that if such degraded craters are used as isopach data points, lava thickness *overestimates* will result because the reduced rim crest is being compared to a fresh (topographically higher) example. This problem is significant where craters have undergone measurable degradation. However, the rate of crater degradation is directly related to the impact flux. Craters over a few kilometers in diameter formed in the last 3.7–3.8 b.y. (during the period of reduced impact flux) have undergone little significant morphologic or morphometric degradation (Head, 1975a). The Imbrium basin formed in the terminal stages of the period of high flux and produced

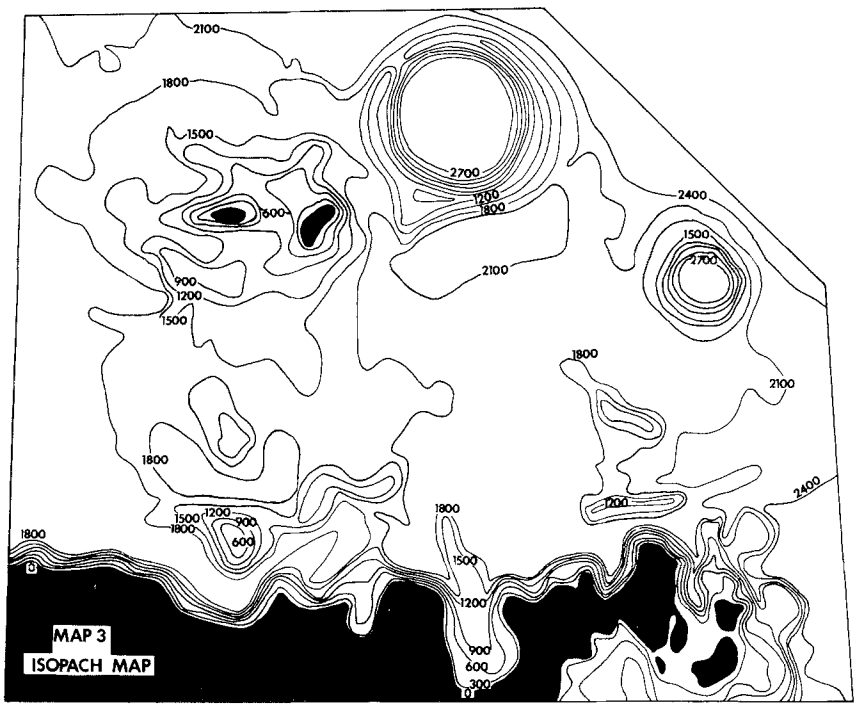

Fig. 9. Isopach map of the Archimedes–Apennine Bench region. Maximum lava thickness is 2.7 km. Isopach interval is 300 m. Black regions are unflooded topography.

TABLE I

Data points for central and Eastern Mare Imbrium from DeHon (1979a) (see Figure 11)

Crater name	Crater diameter (km)
1. Archimedes	84.0
2. Cassini	56.5
3. Lambert R	55.0
4. Wallace	26.0
5. Helicon	24.5
6. Archimedes K (Spurr)	13.2
7. Euler J	3.6

an uncratered surface within the basin. Craters forming subsequently within the basin interior should have undergone little degradation (Head, 1975a); therefore, the question of overestimates raised by Hörz (1978) is probably not applicable within the Imbrium basin. On the other hand, there appear to be several reasons why the technique will produce *underestimates* of lava thicknesses within Imbrium; these reasons are related primarily to normal variations in the rim crest elevation (Settle and Head, 1977).

a)

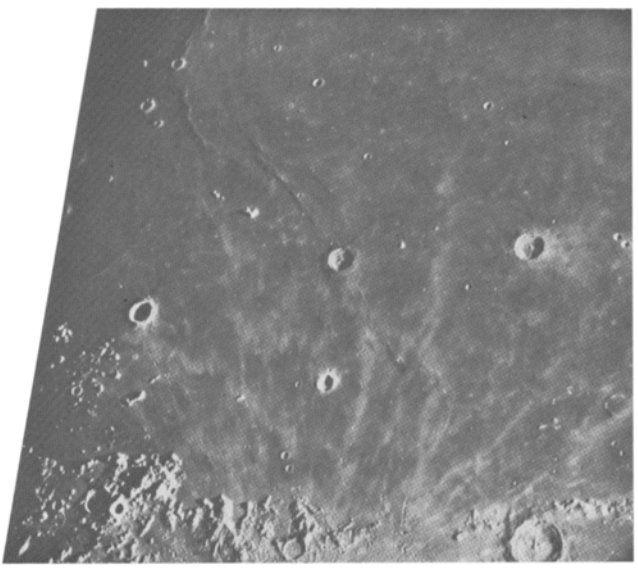

b)

Fig. 10. Earth-based photographs of Imbrium basin. Areas are shown on map in Figure 6a. (a) Area B (C 2699); (b) Area C (C 1911). Photographs are from the Consolidated Lunar Atlas, Supplement Numbers 3 and 4, Lunar and Planetary Laboratory, University of Arizona.

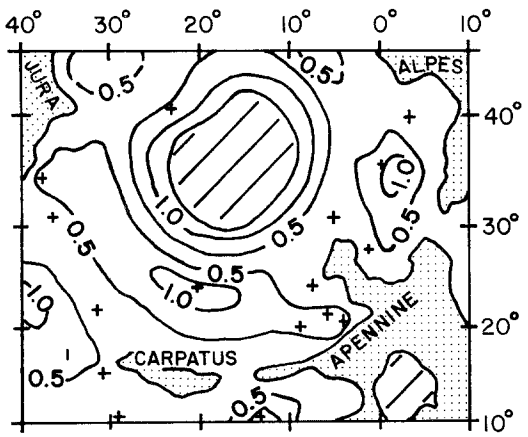

Fig. 11. Isopach map of Mare Imbrium basalt. Isopach interval is 500 meters. Crosses mark the location of measured basalt thickness. Diagonal lines indicate region of unknown values. From DeHon (1979a).

3.2.1. *Rim Heights of Completely Buried Craters*

If a crater is completely buried by lava, its presence can often be detected by a ring of mare ridges or arches which are interpreted to mark the position of the rim crest. The diameter of this ghost crater can then be used to obtain a *minimum* estimate for the thickness of lava. The value of the rim height of the buried crater will *underestimate* the lava thickness for the following reasons: (1) the thickness of lava from the highest point on the buried rim crest to the present mare surface is unknown; (2) even if the thickness is zero (that is, the lava *just covers* the highest point on the rim crest), the rim height value will be an underestimate because it is derived from the *average* value for fresh craters, not the *maximum* value. For example, the fresh crater Autolycus (Figure 8b) is about 40 km in diameter. Topographic data (LM 41) show that its minimum exterior rim height is about 300 m, its maximum value about 1560 m, and an average of these two values is 930 m. The value for an average fresh crater of this diameter (Pike, 1977) is about 960 m. If Autolycus was completely flooded, the thickness of the basalt would be related to its *maximum* rim crest elevation (1560 m), not the average for fresh lunar craters of this size (960 m). For this example, then, the actual lava thickness for the crater buried to the highest point on its rim crest is over 60% greater than the thickness derived from the average rim crest elevation data. Lambert R (Figure 11) is an example of such a ghost crater within Imbrium. The circular ridge structure is approximately 60 km in diameter; a fresh crater of this diameter would have an average rim height of slightly over 1000 m. This value is used by DeHon to define the thickest lava accumulation of the shelf region, a small patch within the 1.0 km isopach contour (Figure 11). On the basis of the above discussion, the Lambert R rim height data point could underestimate the true lava thickness by at least 60%.

3.2.2. *Rim Heights of Incompletely Buried Craters*

If the rim crest of a crater has only been partially buried, the standard approach is to subtract the present rim crest elevation from the average fresh crater value, yielding a lava thickness. However, since the *highest* point on the rim crest is the last rim topography remaining, such a procedure will invariable produce *underestimates* of the true lava thickness. For example, if Autolycus had been flooded to within 100 m of complete submergence of its rim crest, one would derive the following lava thickness [average rim crest elevation (960 m) minus remaining rim crest exposed (100 m) = lava thickness (860 m)]. However, since the highest point on the rim crest is 1560 m, the true lava thickness would be 1460 m, 600 m more than the estimate derived from average values. Thus, normal variation in the topography of crater rim crests can result in *underestimates* of lava thicknesses for partially buried craters.

3.3. PRE-MARE NATURE OF IMPACT CRATER DATA POINTS

A basic assumption of the crater morphometry/mare thickness technique is that the impact crater *predates* the mare flooding episode. Obviously, data derived from any crater *postdating* the onset of mare fill will yield an *underestimate* of lava thickness; the magnitude of the underestimate is related to the time of crater formation relative to stage of mare fill. Late-stage craters will yield the largest *underestimates*. If the average thickness of lava in Imbrium were one km, then only the pre-flooding craters greater than about 50 km diameter would be exposed today. All craters *less* than 50 km in diameter (exterior rim heights of less than 1000 m) should be buried if they predate the emplacement of lavas. It follows that virtually all craters less than 50 km in diameter present on such a surface, formed either *during* or *after* lava emplacement. The thickness estimates developed in this paper *exceed* the one km average value assumed here (about 1.9 km average thickness). DeHon's (1979a, c) average thickness values are *less than* the one km value in the area under consideration (Figure 11), but are derived from the crater data points listed in Table I. The majority of these data points are for craters less than 50 km diameter. Therefore, if the average thickness is equal to or exceeds one km, these craters formed after the beginning of mare emplacement and thus represent *underestimates* of total lava thickness. For example, the crater Helicon (24.5 km diameter, average fresh crater exterior rim height ~ 860 m) in northwest Imbrium has been partially flooded by mare lavas. Helicon must postdate the formation of Iridum crater (middle-Imbrian; Ulrich, 1969) since it is not degraded by Iridum ejecta. Stratigraphic and tectonic evidence strongly suggest that the majority of lava emplaced in circular mare basins was emplaced in the early stages of fill (early Imbrian) (Solomon and Head, 1980). Therefore, on the basis of stratigraphy and crater morphometry, Helicon is very likely to have formed considerably after the beginning of mare filling.

3.4. INFLUENCE OF PRE-EXISTING TOPOGRAPHY ON LAVA THICKNESS ESTIMATES

In areas with few thickness data points, a regional slope of the pre-lava terrain can produce large uncertainties in average thickness estimates. For example, the pre-mare topography

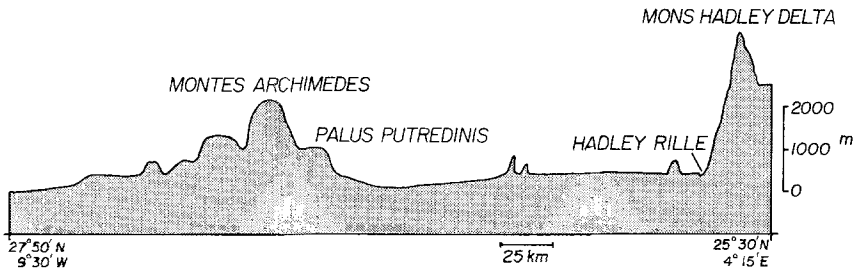

Fig. 12. Topographic profile of the Archimedes–Apennine Bench region prior to artificial flooding. Vertical exaggeration X 20.

between the second and third Imbrian basin rings is relatively low (Figure 12); craters formed on the second ring will therefore initially sit topographically higher than other craters in this part of the basin. If a thickness value derived from such a crater is extrapolated over a large area, a thickness *underestimate* is likely to result. For example, the crater Lambert R is located approximately at the position of the second basin ring. Using the Apennine–Archimedes region as an example, the topography of the ring area may differ from that at the base of the third ring by as much as 1000 m (Figure 12). The DeHon map (Figure 11) shows the lavas thinning from Lambert R to the Carpatus Mountains (third ring). On the basis of the Apennine–Archimedes example, the lavas should *thicken* in this direction, perhaps as much as one kilometer due to the low topography alone. Thus, initial slope of the submare terrain may have an important influence on lava thicknesses in areas with few data points.

On the basis of the above comparisons, it is concluded that the majority of the region between the second and third (Imbrium) rings extending from the Archimedes area around to Oceanus Procellarum exceeds one kilometer average thickness of mare basalts. The area towards the basin interior exceeds this value, as indicated by the Orientale example describe above (Figure 5).

A major question related to the thickness of mare lavas is the importance of *vertical* mixing of material. Rhodes (1977) and Hörz (1978) have discussed the evidence for relatively inefficient lateral transport of highland material onto the mare. To explain the abundance of non-mare fragments in mare soils, Hörz (1978) developed the hypothesis that vertical mixing is significant in bringing sub-mare material to the surface. The mechanism outlined by Hörz is very plausible in areas of relatively thin maria. However, basalt depths 'deeper than 1 km would virtually preclude the vertical admixture of highland materials on the scales observed' (Hörz, 1978, p. 3325). Analysis of the isopach map (Figure 9) shows that only a small portion of the artificially flooded area (~ 10%) is less than one kilometer thick (a small area around the Archimedes Mountain peaks, the rim crest area of Archimedes, and the edge of the Apennine Mountain front). On the basis of this analysis it is concluded that for areas flooded in a manner comparable to the test area, vertical mixing on the scale of the mare regolith is not a significant process.

TABLE II

Basin	Stage I	Stage II
Serenitatis	yes	Part (Outer Rook equivalent).
Humorum	yes	Part (Outer Rook equivalent) plus patchy deposits along megaterrace to East.
Crisium	yes	Part (Outer Rook equivalent) and other minor areas (Patches to E and NE).
Nectaris	part (mostly within inner depression).	Patchy; may be unrelated to Nectaris.
Imbrium	yes	Large part; but outer ring structure uncertain in parts of basin.
Smythii	part (mostly within inner depression).	None?
Grimaldi	part (inner depression only).	None
Orientale	part (inner depression only).	Incipient flooding around base of second and third rings.

4. Discussion and Conclusions

4.1. GEOMETRY OF BASIN FILL

A topographic model of the Orientale basin is used as an approximation of an unfilled basin and is artificially flooded with mare lavas to map the geometry of basin fill. Details in the outer parts of the basin are reconstructed using topographic base maps for the Apennine Bench–Archimedes region of Imbrium. Two stages of fill can be distinguished: Stage I is characterized by flooding of the interior and thick deposits (~ 6 km) of small to intermediate volumes covering small areas (relative to the total basin geometry); Stage II is characterized by flooding out to the basin-defining scarp and thin deposits (~ 2 km) of large volume covering large areas. The resulting fill geometry can be generally approximated by two discs: the Stage II disc radius-to-height ratio exceeds that of Stage I by a factor of five. The concentration of Stage I fill in the basin interior correlates well with the location of the mascon mass in mascon basins. The location of concentric mare ridges may be related to the boundary between the thick and thinner lava load.

The major mascon basins and an interpretation of their flooding geometry are listed in Table II. This table is compiled from geologic maps of the distribution of mare and its relationship to basin ring structure (Wilhelms and McCauley, 1971; Solomon and Head, 1980). All basins show evidence of Stage I flooding, with Orientale, Nectaris, and Smythii having lesser amounts than most other basins. Stage II flooding is not extensive in these basins but often extends to the Outer Rook ring equivalent (second ring) as in the case of

Serenitatis and Humorum. The variable levels of fill are due in part to different states of degradation of the basin topography due both to impact modification and possible viscous relaxation (Solomon and Head, 1981). An additional cause of variation, however, is the different level of development of the ring structure both within and between impact basins (see maps in Solomon and Head, 1980). This initial variation is manifested as poorly developed or discontinuous rings (as in the outer ring of Nectaris) and undeveloped ring topography (as in the outer ring of Crisium). For example, the lack of development of a megaterrace in Crisium comparable to the one in Orientale enhanced the topography of the second ring and confined flooding largely to the region within that ring. Thus, for the mascon basins, the geometry of mare fill is a function of initial development of basin structure as well as extent of flooding.

The Orientale basin example provides a model for the geometry of lava fill of lunar basins and a framework for the study of style of lava filling, loading of the lithosphere, deformation of mare surfaces, and the relationship of impact basins to ensuing stages of volcanism. A major variable is the initial state of basin topography and ring development. No basin (even Orientale) is exactly like the Orientale topographic model. Comparison of the Orientale model and stages of development of mare flooding in other basins relative to their structure will provide a better understanding of the significance of this variable. In addition there may be variations between basins relative to the level of thermal stresses associated with basin formation (Bratt *et al.*, 1981) which may influence initial topography.

In summary, the application of the Orientale basin model to other basins should be done carefully, considering the following factors which might cause *overestimates* (different initial basin geometries in early lunar history caused by different target characteristics or variations in isostatic readjustments; degradation and infilling by impact processes) or *underestimates* (loading of the lithosphere by early basin fill, and subsidence of the basin floor).

4.2. SEQUENCE OF BASIN FILL

The Orientale model of basin flooding assumes that flooding begins at the lowest point in the basin and proceeds topographically upwards until flooding is complete. Studies of mare deposites in the partly flooded Orientale basin (Greeley, 1976; Gaddis and Head, 1981) show them to be concentrated as a large patch on the lowest part of the basin floor and also as small arcuate lakes along the base of the scarps defining the outer Rook and Cordillera rings. The fact that these latter lakes occur several kilometers above the basin floor mare deposit indicates that the modelling procedure is a simplification: in Orientale multiple vents exist at different elevations within the basin.

Other basins, however, provide clues to the nature of early volcanic fill more extensive than that found in Orientale. Stratigraphic studies of the deeply flooded maria Serenitatis (Howard *et al.*, 1973) and Crisium (Head *et al.*, 1978) show that the oldest deposits are exposed around the outermost edge of the maria deposits. Stratigraphic relationships and material excavated by impact craters confirm the presence of this early fill in the central maria, underlying thinner, younger deposits.

The thick accumulation of early lava fill in the basin interior as indicated by observations and the Orientale flooding model causes loading of the lithosphere resulting in flexure and deformation of the newly emplaced deposit (Solomon and Head, 1979; 1980). This downwarping may exceed one to two km in the central part of the basin.

4.3. VERTICAL MIXING

Efficient vertical mixing of sub-mare material requires lava thicknesses of less than one km (Hörz, 1978). On the basis of this analysis, vertical mixing would be precluded in virtually all regions of Stage I flooding and in any areas of extensive Stage II flooding of basins, such as the southern part of Mare Imbrium. Vertical mixing is not precluded in very shallow parts of basins (< 1 km thick) and in other shallow areas outside basins.

4.4. ISOPACH MAPS COMPILED ON THE BASIS OF EXTERIOR RIM HEIGHTS OF FLOODED CRATERS

Several lines of evidence are developed that show that standard techniques of isopach map compilation may introduce errors which seriously underestimate and overestimate lava thicknesses. Overestimates can be caused by crater degradation, whereas underestimates can be caused by normal variations in crater rim crest topography and by the use of craters that postdate the beginning of mare fill. These problems are exacerbated when only a small number of data points is available. On the basis of these considerations, previous estimates for lava thicknesses in Imbrium (DeHon, 1979) are believed to underestimate true thicknesses by more than a factor of two.

Acknowledgements

This work was supported by National Aeronautics and Space Administration grant NGR-40-002-088 from the Planetary Geology Program. Edmund Robinson developed the programs used in the lava flooding of topography. Ruth Gorski and Suzanne Church drafted the figures. Suzanne Church, Nancy Christy, Sally Bosworth, and Susan Sharpton aided in preparation of the manuscript. Mark Cintala and James L. Whitford-Stark provided helpful reviews of the manuscript.

Appendix A

Data reduction is accomplished in four steps: digitization, derotation, matrix assignment and area-volume calculations. The equipment used is a Talos Cybergraph digitizing board, Tektronix 4051 microprocessor, and IBM 370/138 computer.

The digitizing procedure is as follows: First, the contour intervals on each map were color coded in increments of 300 m. The maps were then fastened to the digitizing board; the corners, scale and contour lines were digitized. As each position value came in from the board, it was derotated (i.e., the tilt of the map with respect to the board coordinate system was removed) and the data points were recorded on tape. The rate of data sampling

on each contour line was about 3 per second. At the end of a session, the data created by the program was transferred to an IBM compatible tape.

The tape was used as input to a program called MATRIX which calculates the position of a contour height value in a 100 x 100 element matrix, the area represented by individual matrix elements, and finally a smoothed version of the matrix. The position of the height value is calculated by subtracting the offset x, y value from the position x, y value, dividing the results by the total x, y length of the map, and multiplying the result by 100. In case of multiple values occupying the same matrix element, the highest value is chosen. The matrix is smoothed by finding two nonzero elements with zero value elements between them, the value placed in the zero element is computed by linear interpolating of the two nonzero points. Area of each element is computed by determining the length (Row S column) value in kilometers of each element, and multiplying them together.

The final data reduction program (MATCLC) calculates the area covered and the volume of the emplaced lava. The program allows up to forty different lava fill height values to be input. The height value of interest is subtracted from the height value in a matrix element. If the difference is negative or zero, the element is considered 'not filled' and a new element is chosen. If positive, the element is considered filled, the area of that element is added to the total fill area, the difference in heights is multiplied by the element area, and this volume element is added to the total volume of emplacement lava. Elements of the matrix are checked once for each contour height of interest, and the results are printed and plotted.

References

Andre, C. G., Wolfe, R. W., Adler, I., and Clark, P. E.: 1979, *Lunar and Planet. Sci.* **X**, 38.

Baldwin, R. B.: 1970, *Publications of the Astron. Soc. of the Pac.*, **82**, 857.

Bratt, S. R., Solomon, S. C., and Head, J. W.: 1981, *Lunar and Planet. Sci.* **XII**, 109.

Brown, W. E., Adams, G. F., Eggleton, R. E., Jackson, P., Jordan, R., Kobrick, M., Peeples, W. J., Phillips, R. J., Porcello, L. J., Schaber, G., Sill, W. R., Thompson, T. W., Ward, S. H., and Zelanka, J. S.: 1974, *Proc. Lunar Sci. Conf. 5th*, 3037–3048.

Cooper, M. R., Kovach, R. L., and Watkins, J. S.: 1974, *Rev. Geophys. Space Phys.* **12**, 291.

DeHon, R. A.: 1974, *Proc. Lunar Sci. Conf. 5th*, 53–59.

DeHon, R. A.: 1975, *Proc. Lunar Sci. Conf. 6th*, 2553–2561.

DeHon, R. A. and Waskom, J. D.: 1976, *Proc. Lunar Sci. Conf. 7th*, 2729–2746.

DeHon, R. A.: 1977, *Proc. Lunar Sci. Conf. 8th*, 633–641.

DeHon, R. A.: 1979a, *Lunar and Planet. Sci.* **X**, 271.

DeHon, R. A.: 1979b, *Lunar and Planet. Sci.* **X**, 274.

DeHon, R. A.: 1979c, *Lunar and Planet, Sci.* **X**, 2935.

Gaddis, L. R. and Head, J. W.: 1981, *Lunar and Planet. Sci.* **XII**, 321.

Greeley, R.: 1976, *Proc. Lunar Sci. Conf. 7th*, 2747–2759.

Greeley, R. and Womer, M. B.: 1980, *Lunar and Planet. Sci.* **XI**, 362.

Grieve, R. A. F., Dence, M. R., and Robertson, P. B.: 1977, in Roddy, D. J., Pepin, R. O., and Merrill, R. B. (eds.), *Impact and Explosion Cratering*, Pergamon Press, New York, 791–814.

Hawke, B. R. and Head, J. W.: 1978, *Proc. Lunar Planet. Sci. Conf. 9th*, 3285–3309.

Head, J. W.: 1974a, *Geochim. Cosmochim. Acta Suppl.* **5**, 207.

Head, J. W.: 1974b, *The Moon* **11**, 327.

Head, J. W.: 1975a, *The Moon* **12**, 299.

Head, J. W.: 1975b, *Rev. Geophys. Space Phys.* **14**, 265.
Head, J. W., Settle, M., and Stein, R. S.: 1975, *Proc. Lunar Sci. Conf. 6th*, 2805–2829.
Head, J. W.: 1978, *The Moon and the Planets* **21**, 439.
Head, J. W., Adams, J., McCord, T., Pieters, C., and Zisk, S.: 1978, in Merrill, R. B. and Papike, J. J. (eds.), *Mare Crisium: The View From Luna 24*, Pergamon Press, New York, 43–74.
Head, J. W.: 1979a, *Lunar and Planet. Sci.* **X**, 516.
Head, J. W.: 1979b, *Lunar and Planet. Sci.* **X**, 519.
Head, J. W., Robinson, E., and Phillips, R.: 1981, *Lunar and Planet. Sci.* **XII**, 421.
Hörz, F.: 1978, *Proc. Lunar Sci. Conf. 9th*, 3311–3332.
Howard, K., Carr, M., and Muehlberger, W.: 1973, *NASA SP-330*, p. 31–22 to 31–25.
Howard, K. A., Wilhelms, D. E., and Scott, D. H.: 1974, *Rev. Geophys. Space Phys.* **12**, 309.
Kaula, W. M., Schubert, G., and Lingenfelter, R. E.: 1974, *Proc. Lunar Sci. Conf. 5th*, 3049–3058.
Marshall, C. H.: 1961, *U.S. Geol. Surv. Prof. Pap. 424-D*, 208–211.
Maxwell, T. A. and Phillips, R. J.: 1978, *Geophys. Res. Lett.* **5**, 811.
Moore, H. J., Hodges, C. A., and Scott, D. H.: 1974, *Proc. Lunar Sci. Conf. 8th*, 1383–1415.
Peeples, W. J., Sill, W. R., May, T. W., Ward, S. H., Phillips, R. J., Jordan, R. L., Abbott, E. A., and Killpack, T. J.: 1978, *J. Geophys. Res.* 77, 7106.
Phillips, R. J., Conel, J. E., Abbott, E. A., Sjogren, W. L., and Morton, J. B.: 1972, *J. Geophys. Res.* 77, 7106.
Pike, R. J.: 1977, in Roddy, D. J., Pepin, R. O., and Merrill, R. B. (eds.), *Impact and Explosion Cratering*, Pergamon Press, New York, 489–509.
Pike, R. J.: 1978, *U.S. Geol. Surv. Prof. Pap. 1046-C.*
Rhodes, J. M.: 1977, *Phil. Trans. R. Soc. London* **A285**, 293.
Scott, D. H., McCauley, J. F., and West, M. N.: 1977, 'Geologic Map of the West Side of the Moon', *U.S. Geological Survey Map I-1034*.
Settle, M. and Head, J. W.: 1977, *Icarus* **31**, 123.
Settle, M. and Head, J. W.: 1979, *J. Geophys. Res.* **84**, 3081.
Sharpton, V. L. and Head, J. W.: 1980a, *Lunar and Planet. Sci.* **XII**, 964.
Sharpton, V. L. and Head, J. W.: 1980b, *Lunar and Planet. Sci.* **XII**, 961.
Solomon, S. C. and Head, J. W.: 1979, *J. Geophys. Res.* **84**, 1667.
Solomon, S. C. and Head, J. W.: 1980, *Rev. Geophys. Space Phys.* **18**, 107.
Solomon, S. C. and Head, J. W.: 1981, *Lunar and Planet. Sci. Conf.* **XII**, 1023.
Spudis, P. D.: 1978, *Proc. Lunar and Planet. Sci. Conf. 9th*, 3379–3394.
Talwani, M., Thompson, G., Dent, B., Kahle, H., and Buck, S.: 1973, *Apollo 17 Prelim. Sci. Rept., NASA SP-330*, 13–1 to 13–13.
Thurber, C. H. and Solomon, S. C.: 1978, *Proc. Lunar Sci. Conf. 9th*, 3481–3498.
Ulrich, G. E.: 1969, 'Geologic Map of the J. Herschel Quadrangle of the Moon', *U.S. Geological Survey Map I-604*.
Watts, C. B.: 1963, Astron, Pap. Ephem. 17, USGPO, Washington, D.C.
Wilhelms, D. E. and McCauley, J. F.: 1971, 'Geologic Map of the Near Side of the Moon, 1:5 000 000', *U.S. Geological Survey Map I-703*.
Womer, M. B. and Greeley, R.: 1980, *NASA TM-81776*, 210–212.